DOI: 10.13009/EUCASS2019-444

Efficiency of the thermal energy storage made of lunar regolith

Marianna Fulara and Karol Seweryn***

**Warsaw University of Technology (WUT), Pl. Politechniki 1, 00-661 Warsaw, Poland,*
** Space Research Centre of the Polish Academy of Sciences (CBK PAN), Bartycka 18a, 00-716 Warsaw, Poland,*
Email: majka.wasilewska@gmail.com

*** Space Research Centre of the Polish Academy of Sciences (CBK PAN), Bartycka 18a, 00-716 Warsaw, Poland,*
Email: kseweryn@cbk.waw.pl

Abstract

In this paper, the possibility to determine the parameters of a thermal energy storage material in order to maximize the efficiency of its heating process in the lunar environment was confirmed. Using simulation analyzes, the influence of parameters such as thermal conductivity, specific heat of the storage material and thermal contact conductivity at the storage boundary on the temperature achieved in the storage and its heating time is shown. Then, the efficiency of heating process by means of two coefficients was examined. At the end, simple experimental tests were carried out.

1. Introduction

Mankind have been exploring the Earth for centuries and there is less and less to discover, so we're turning our eyes to further corners of the universe. For over 70 years, we have been sending instruments into space that provide a lot of data about the Earth and outer space. In addition to satisfying curiosity, space exploration also brings other benefits such as scientific and technological development, economic expansion, building international cooperation or inspiring next generations to choose engineering professions.

The goals of space exploration set by space agencies from around the world in the document *The Global Exploration Strategy* [1] are a manned flight to the Moon, the first human flight to Mars, the study of the moons of further planets and asteroids, and in the long run, the establishment of permanently inhabited outposts on the Moon and Mars. To achieve all this, it is necessary to develop a number of technologies such as sensors, biochemical technology and the In-Situ Resources Utilization (ISRU).

ISRU is intended to reduce the mass, cost, and risk of robotic and human exploration [2]. Planetary resources that can be used are for example water, metals and minerals, solar wind implanted volatiles, atmospheric constituents or even solar energy [3].

Four ISRU stages are defined [4]

a. Reconnaissance, prospecting and mapping – first, reconnaissance carried out by means of satellites and then by in-situ tests. The goal is to identify areas with the highest abundance and availability of resources in terms of mission consumables (such as water and fuel) and creating its maps. It is necessary to study not only the regolith, but also the atmosphere and the environment.

b. Resource acquisition – this includes the extraction and collection of materials and their preliminary processing and storage of raw resources. Such actions have not yet taken place on a large scale outside the Earth.

c. Processing and production – it will be necessary to extract solid, liquid and gaseous substances by means of thermal, chemical, catalytic and electric processes from the materials obtained.

d. Manufacturing products and infrastructure emplacement – this stage includes production of infrastructure, as well as tools that will be needed for the outpost and for the safety of crew and robots. For example the landing pads, habitats or roads will be required as well as systems for the supply of heat and electricity (such as *Thermal Wadi* or Thermal Energy Storage).

DOI: 10.13009/EUCASS2019-444

One of the needs that will arise when designing long-term lunar missions is to provide people and infrastructure (e.g. rovers, habitats, transportation or life support systems) with energy for a long and harsh lunar night. Solar energy is then not available and the temperature drops below -150°C. This is dangerous for people as well as any mechanical or electrical devices working there. For example the typical rover onboard computer have temperature limit equal to -55°C.

Systems such as Thermal Wadi [5,6] were analyzed for night heating of rovers and Thermal Energy Storage (TES) [7] for generating electricity for the needs of a manned outpost. An important advantage of these energy storage systems is the possibility to create thermal masses from modified lunar regolith. Modifications such as compression, melting or sintering have been proposed in [8] to obtain a solid mass with suitable thermal properties.

In this work the analysis of the efficiency of the thermal mass heating process depending on its thermal parameters such as thermal conductivity or specific heat was made. In next two subsections the details about lunar environment and problem statement is provided. In next section description of the thermal energy storage model and the analyzes of the achieved temperature and heating time depending on the material parameters carried out on it are presented which are followed by study of the efficiency of the heating process and experimental tests. Finally in conclusions the summary of paper is given.

1.1 Lunar environment

Important parameters for solar thermal storage systems is the time and intensity of illumination of potentially suitable areas and changes in temperature on these places.

The inclination of the Moon's orbit is small as is the inclination of its equatorial plane to the plane of the ecliptic. Periods of circulation around the Earth and the rotation of the Moon are synchronized and amount to 27.3 Earth days, so the Moon is always facing the same side to Earth. This results in the time of illumination of particular areas on the Moon - in the equatorial regions, day and night last about two weeks, while at poles there are areas where incident radiation is constant, but at a very high angle. This impact the temperature diurnal cycle which extremes are presented in table 1.1.

Table 1.1: Temperatures on the surface of the Moon [9]

	Shadowed polar craters	Other polar areas	Equatorial areas	Typical mid-latitudes
Average temperatures	40 K	220 K	255 K	220<T<255 K
Monthly range	-	+/-10 K	+/-140 K	+/-110 K

Regolith covers over 99% of the Moon's surface with a layer of several to tens of meters thick. It is formed mainly by continuous bombardment of meteorites of very different sizes, which cause comminution, agglutination and mixing of material. This makes the native regolith consist of very fine particles (95%wt is composed of granules smaller than 1mm, 50%wt - smaller than 50μm [9]) with irregular shapes and has a high porosity (40-50%) [9], and low thermal conductivity. Studies indicate that even a small amount of regolith causes temperature wave attenuation.

1.2 Problem statement

The system TES analyzed in [7] is used to provide electricity to manned outpost during the lunar night. A set of concentrators focuses the radiation on the Loop Heat Pipe - LHP, in which the heated working fluid flows. It transports energy to the thermal mass hidden under the ground. From there, energy is delivered to the heat engine. On the other side of heat engine, the remaining energy is transported to the radiator placed on the surface and shielded from solar radiation.

This paper deals with the analysis of thermal mass made of modified regolith. The thermal mass is located under the surface of the Moon and surrounded by a native regolith. Energy is supplied by the heater placed in the mass axis, part of the energy is lost to the environment and part is to be transferred to the Stirling engine during the lunar night. These processes are shown in the Figure 1.1.

DOI: 10.13009/EUCASS2019-444

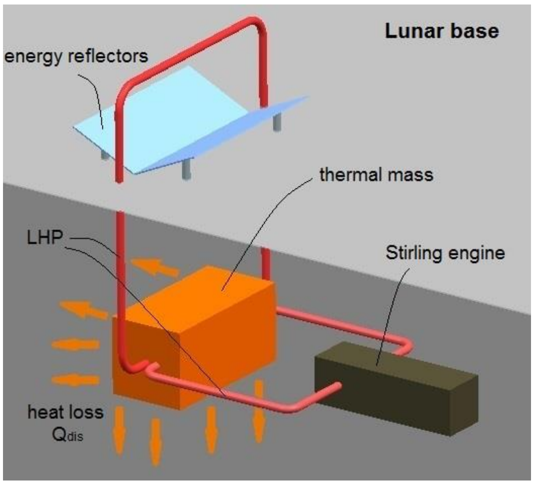

Figure 1.1: Processes to which the thermal mass is subjected.

The thermal mass is under the surface of the lunar soil. It is made of regolith modified by, for example, the microwave sintering method [8], to create a solid mass with better thermal parameters than native regolith. Inside the mass there is an LHP in the hole drilled, for example by the directional drilling method. During the lunar day, the fluid heated by solar radiation flows into the thermal mass. The mass gradually warms up, but some energy is dissipate to the surrounding native regolith, which reduces the heating efficiency.

This paper confirms the possibility of determining the optimal parameters of the thermal energy storage material allowing for the maximization of the efficiency of the heating process of the storage in lunar conditions. A number of assumptions regarding environmental conditions and material parameters were made based on the TES system study [7]. Analyzes are carried out for the worst case of storage location – that is, in the equatorial region, where the lunar night and day last for two weeks each. The system consists of the material of the storage surrounded by the native regolith and heated by a heater that simulates part of the LHP was analyzed. The research was based on simulation analyzes and experimental tests.

2. Theoretical model

The simulations were performed on a model that includes:

- a rectangular heater with a base side of 100mm length, made of a material with the properties of basalt rock representing modified regolith [7] (domain 1, fig. 2.1),
- energy storage, with a base side 500mm long – also with basalt rock properties (domain 2, fig. 2.1)
- material surrounding the storage with the base side 1000mm long and with the properties of native regolith (domain 3, fig. 2.1).

To minimize the computational cost, the symmetry of the model with respect to the z-axis was used and the simulations were performed at 0.25 of the cross-section of the energy store and its surroundings - fig. 2.1.

DOI: 10.13009/EUCASS2019-444

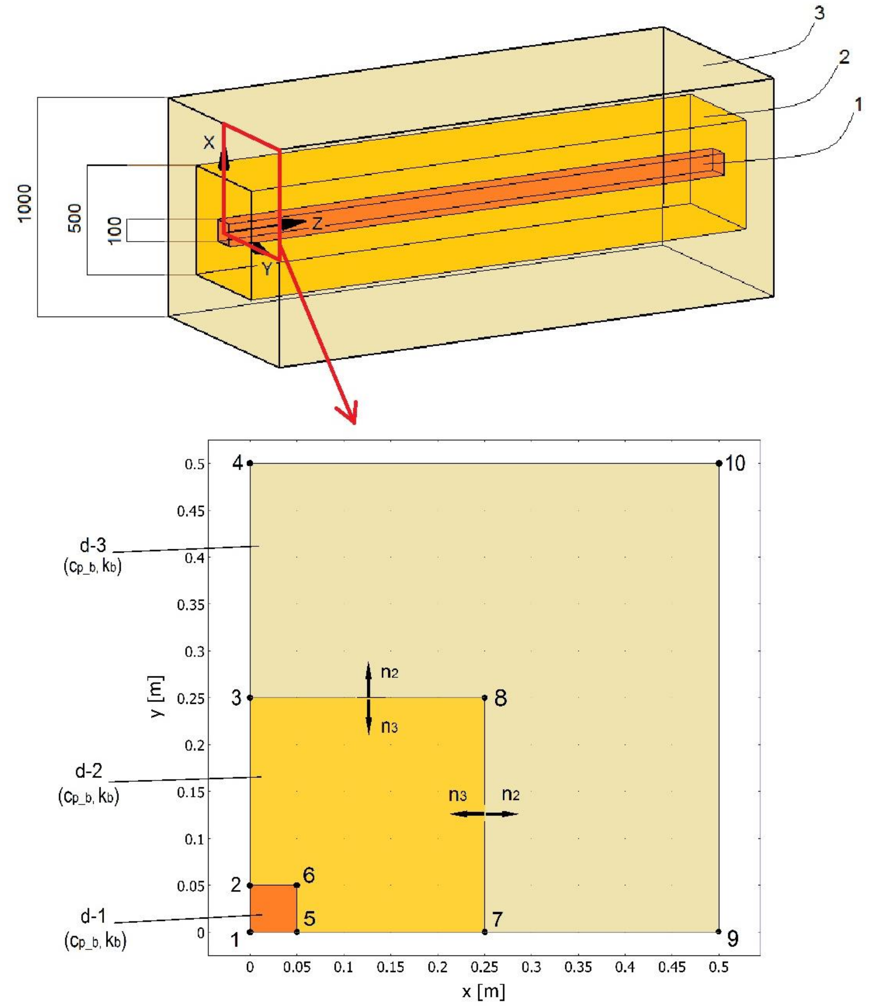

Figure 2.1: Model geometry, d-1 – heating element and d-2 – energy storage with modified regolith properties, d-3 – material surrounding the storage with native regolith properties.

Properties of the materials used are presented in Table 2.1.

Table 2.1: Parameters of materials according to [7]

Parameter	Native regolith	Basalt rock
Density	$\rho_r = 1800[kg/m^3]$	$\rho_b = 3000[kg/m^3]$
Specific heat	$c_{p\_r} = 840[J/(kgK)]$	$c_{p\_b} = 800[J/(kgK)]$
Thermal conductivity	$k_r = 0.01[W/(mK)]$	$k_r = 2.1[W/(mK)]$
Thermal contact conductivity between basalt rock and native regolith	$h_j = 5[W/(m^2K)]$	

The heat generated by the heater is absorbed and stored in a thermal mass so that it can be converted into electricity at the right time. The heat received from the heating element in the storage propagate by conduction in the *x* and *y* directions, taking into account the temperature distribution, heat flows in these two dimensions describe the equations:

$$q_y = -k_y \frac{\partial T}{\partial y}, \qquad q_y = -k_y \frac{\partial T}{\partial y} \tag{2.1}$$

where q_x, q_y [W/m^2] are heat flows in appropriate directions, a k [$W/(mK)$] is the coefficient of thermal conductivity of the material.

To calculate the temperature distribution in the model, the Fourier-Kirchhoff law is used by means of equation (2.2).

DOI: 10.13009/EUCASS2019-444

$$\rho c_p \frac{\partial T}{\partial t} + k\nabla(-\nabla T) = Q \qquad (2.2)$$

where ρ is the density, c_p – specific heat, Q - generated heat ($Q\neq 0$ only for 1. domain (heater), for 2. and 3. domains $Q=0$).

At the interface of modified and native regolith (domains 2 and 3) the thermal contact resistance was taken into account by means of equations:

$$-n_2(-k_b\nabla T_2) = q_0 + h(T_3 - T_2) \qquad (2.3)$$

$$-n_3(-k_r\nabla T_3) = q_0 + h(T_2 - T_3)$$

where n - (fig. 2.1) normal to the external surface of the domain – represented by lines between points 7-8 and 8-3 (fig. 2.1), T - contact surface temperature for the domain, and k_b, k_r - coefficients of thermal conductivity of basalt rock and native regolith (table 2.1), h – thermal contact conductivity between basalt rock and native regolith.

Then heat propagate in the native regolith according to Fourier-Kirchhoff's law.

The vertices of the model are marked with numbers from 1 to 10. These points will be used in the simulations.

For the simulations on the above-described model the MATLAB and COMSOL Multiphysics (Heat Transfer Modul) software were used. The influence of changes in parameters such as thermal conductivity and specific heat of the material from which the storage will be constructed or thermal contact conductivity at the interface between the store and its surroundings on the energy storage's properties – the temperatures reached, the heating time and the efficiency of the heating process are illustrated.

3. Results

A series of simulations were carried out in parallel to investigate the influence of change in thermal contact conductivity at the interface of modified and native regolith, thermal conductivity and specific heat of thermal mass material and heater power on the temperature distribution in the system and time and efficiency of the heating process.

3.1 Temperature distribution in the heated system depending on the boundary condition

Simulations were carried out with a constant and transient temperature condition at the edge of the model. The transient boundary condition is to imitate the temperature changes on the surface of the Moon. The obtained temperature distributions were compared to check the effect of radiation on the surface on the temperature in the storage.

The initial temperature in both simulations is $T_0=100K$, and the assumed simulation time $t=1.2744e6[s]=354h$ [7]. The temperature at the edge of the model for the first simulation is also $T=100K$, the temperature distribution obtained at the end of time is shown in fig. 3.1.

In the second simulation, the temperature at the edge of the native regolith is described by the equation (3.1) (after [7] it rises to 177 hours and then falls):

$$T_{time} = 110 + 60\frac{solarflux(t)}{1300} \qquad (3.1)$$

where:

$$solarflux(t) = 1300\sin\left(\frac{\pi t}{1274400}\right)$$

The obtained temperature distribution for subsequent time moments is shown in Fig. 3.2.

DOI: 10.13009/EUCASS2019-444

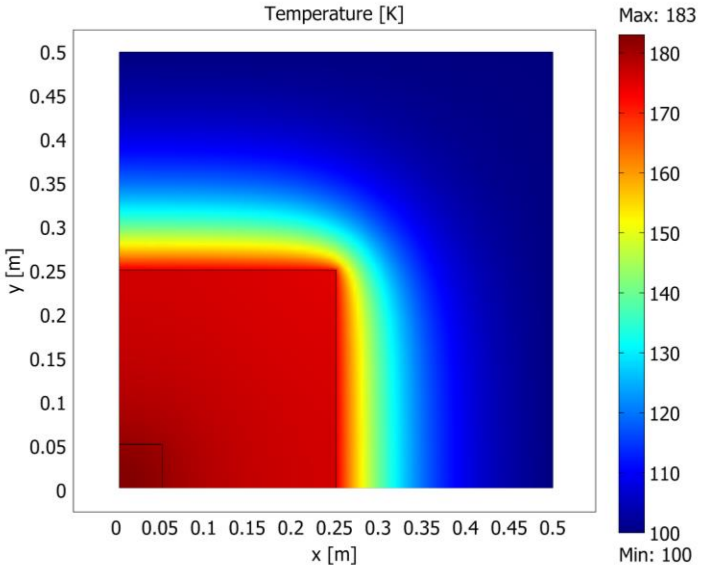

Figure 3.1: Temperature distribution at the end of time for simulations with constant temperature on the edge of the model.

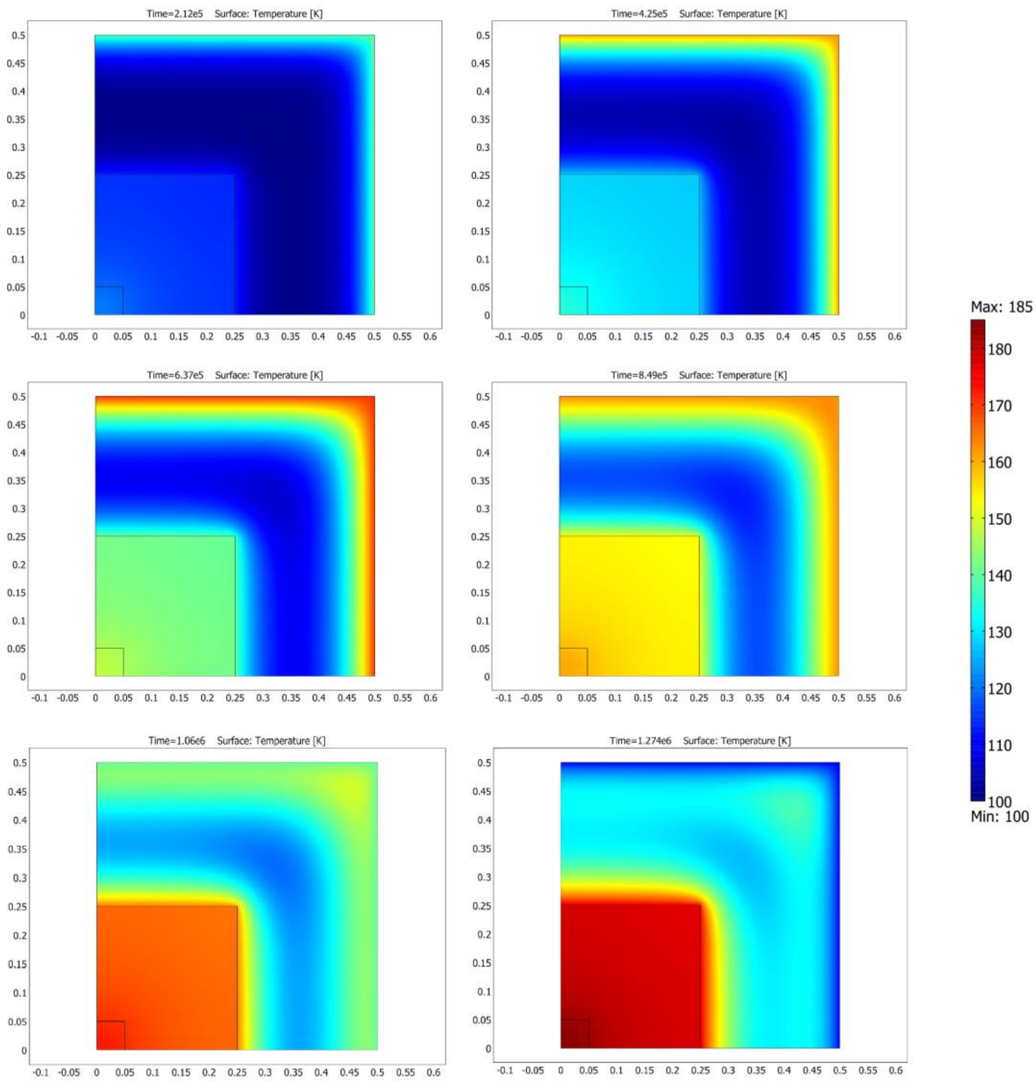

Figure 3.2: Temperature distribution for subsequent moments of time in a model with a transient boundary condition.

DOI: 10.13009/EUCASS2019-444

Similar simulations were carried out for three heater power values:

- *5000 W/m³* (minimum power needed to heat a similar energy storage);

- *33333 W/m³* (power needed to obtain about 1000K in the storage, that is needed to run the Stirling engine if the storage is used as a hot side [7]) ;

- *60000 W/m³* (the power assumed is large enough to illustrate the changes occurring in the temperature distribution in the model).

Then the temperature in point 8. for the modified regolith (T2) was read for the end time, half of that time and its one quarter for three values of the heater's power. These results were compared for simulations with constant and time-dependent boundary conditions, the latter being slightly higher. Differences are presented in table 3.1.

Table 3.1: Comparison of temperatures obtained in point 8. in simulations with constant and time-dependent boundary condition

	Q=5000 [W/m³]	Q=33333 [W/m³]	Q=60000 [W/m³]
¼ t	0.064 [K]	0.088 [K]	0.106 [K]
½ t	0.176 [K]	0.024 [K]	0.101 [K]
t	1.384 [K]	1.177 [K]	1.208 [K]

Temperature differences between two boundary conditions are small – they do not exceed 1.5K, which confirms that the native regolith insulates the storage from the external temperature conditions well.
This study also indicates that some of the energy dissipates to the surrounding regolith despite the difference in thermal conductivity and thermal contact resistance.

3.2 Influence of the thermal contact conductivity values at the interface of the energy storage and native regolith *h* to the temperature distribution

Point 8 (fig 2.1) is located on the interface between the energy storage and native regolith materials. This is the point in the storage as far as possible from the heater, so the temperature at this point is also the minimum temperature in the energy storage.

Temperature values were generated in point 8. for the energy storage (T_2) and the environment (T_3 – the native regolith) at the final simulation time for the heating element's power values in the range from *5* to *100* [kW/m^2] for two thermal contact conductivity values – $h=5[W/(m^2K)]$ and $h=0.5[W/(m^2K)]$. The results are shown in Figure 3.3.

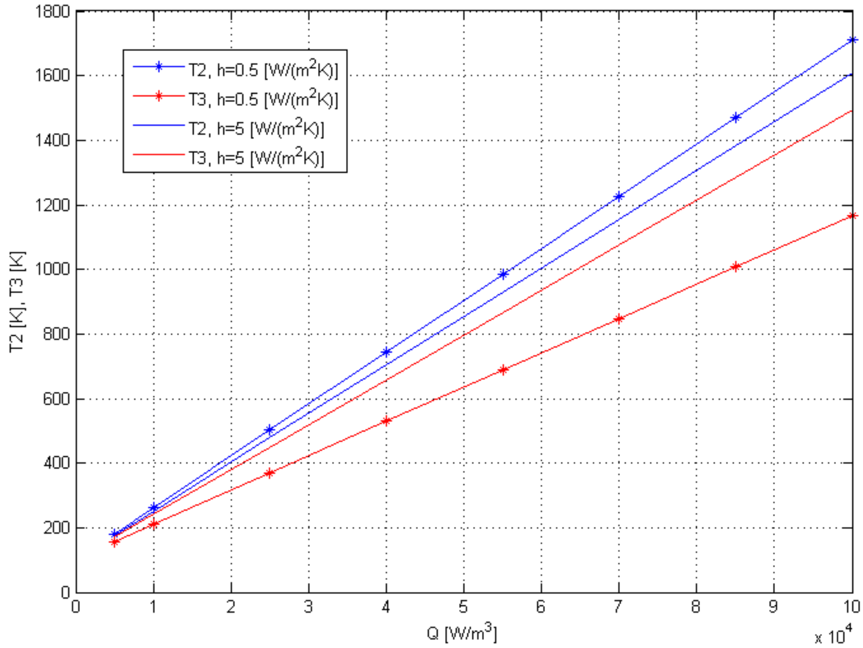

Figure 3.3: Temperatures in point 8. by modified (T_2) and native regolith (T_3) for different values of heat generated by the heater and two values of thermal contact conductivity *h*.

DOI: 10.13009/EUCASS2019-444

In figure 3.3, smooth lines show temperature changes in point 8. for *h=5[W/(m²K)]*, while lines with markers for *h=0.5[W/(m²K)]*. The reduction of the thermal contact conductivity results in an increase of the temperatures reached in the energy storage and a fall in the temperature in the native regolith at the same point, and thus an increase in the temperature difference between the modified and native regolith. It follows that the smaller *h* (and the greater the thermal resistance at the material interface) can be achieved, the more heat will be deposited in the energy storage.

3.3 The influence of thermal parameters on the required power of the heater *Q*

Analyzes of the power needed to heat the storage were carried out. For the previously used three values of the heater's power (*5000, 33333, 60000W/m³*), temperature changes depending on time at point 7 were read (fig 2.1) for the modified and native regolith and are shown in the diagram (fig. 3.4).

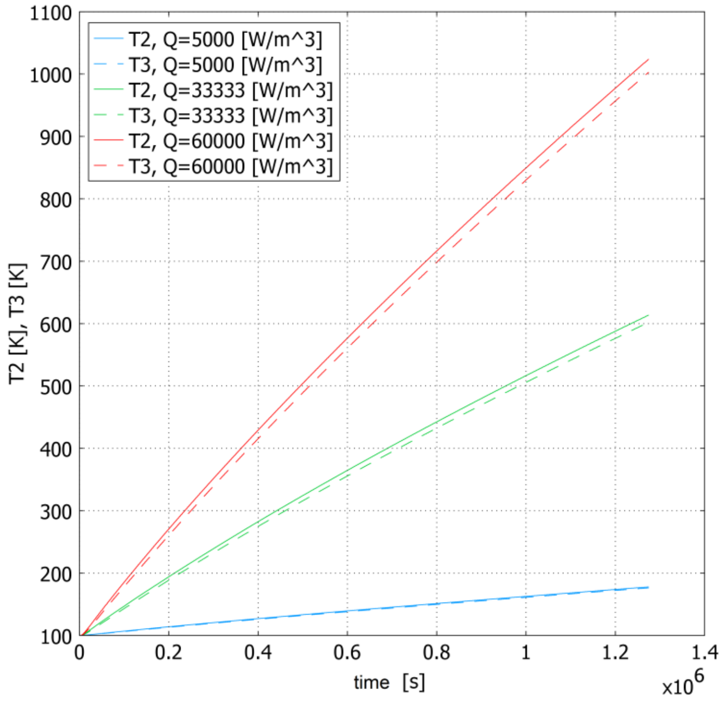

Figure 3.4: Diagram of modified (*T2*, solid lines) and native regolith (*T3*, dashed lines) temperatures in point 7. for different values of heater power.

It is visible that the higher the heater's power, the higher temperature values reaches the energy storage and the temperature differences between the modified and native regolith are larger. Numerical values (T_2-T_3) are given in Table 3.2.

Table 3.2: Temperature values in point 7. for different heating element's power.

Power [W/m^3]	Maximum temperature [K]	Temperature of the modified regolith in point 7 [K] (T_2)	Temperature of the native regolith in point 7 [K] (T_3)	T_2-T_3 [K]
5000	182.92	176.57	174.81	1.76
33333	654.73	612.36	600.59	11.77
60000	1098.68	1022.41	1001.22	21.19

Only for a power of *60000W/m³*, the storage reaches a temperature of 1000K during the lunar day.

DOI: 10.13009/EUCASS2019-444

It was also examined what is the influence of changes in the specific heat value of the storage material on the required power. For this purpose, diagrams of the time needed to heat the extreme point in the energy storage (point 8. fig. 2.1) were generated by 10, 100 (auxiliary values) and 1000K (required at the end of the lunar day in the storage to drive the Stirling engine at night) from the power of heater. Figure 3.5 shows the values for the specific heat of the storage material c_{pb}*=800[J/(kgK)]*, and Figure 3.6 for c_{pb}*=80[J/(kgK)]*.

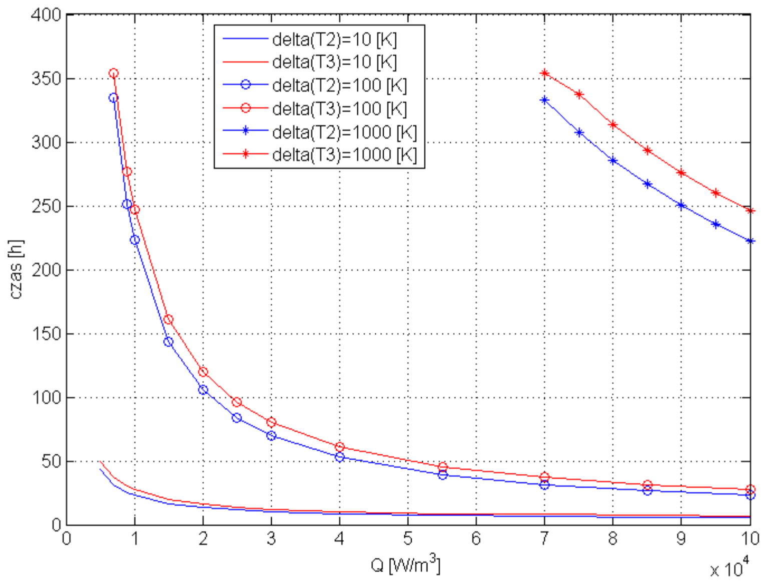

Figure 3.5: Time needed to heat modified (*T2*) and native (*T3*) regolith at point 8. by 10K (smooth lines), 100K (lines marked with circles), 1000K (lines marked with asterisks) for different values of heat generated by the heater and values of specific heat of the modified regolith c_{pb}*=800[J/(kgK)]*.

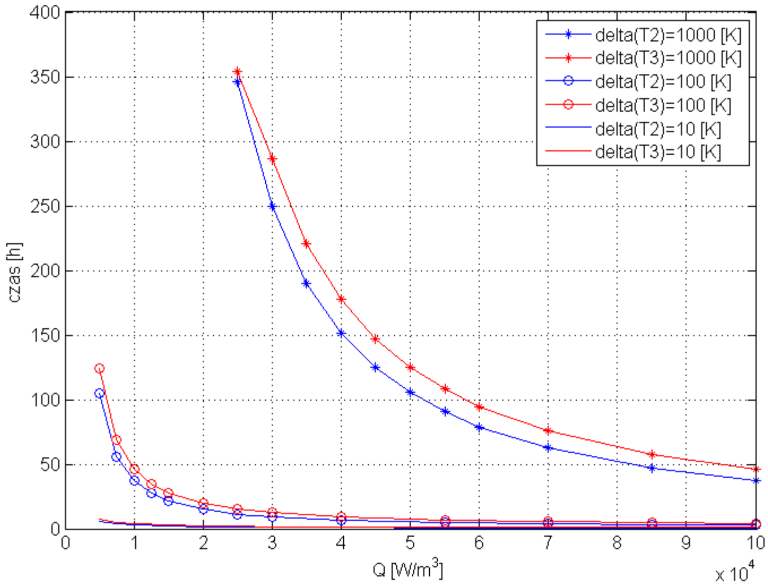

Rys 3.6 Time needed to heat modified (*T2*) and native (*T3*) regolith at point 8. by 10K (smooth lines), 100K (lines marked with circles), 1000K (lines marked with asterisks) for different values of heat generated by the heater and values of specific heat of the modified regolith c_{pb}*=80[J/(kgK)]*.

For c_{pb}*=800[J/(kgK)]* (Figure 3.5) the storage in point 8. warm up by *100K* during the lunar day from the heater's power of about *7[kW/m*^{3}*]*, whereas by *1000K* it is only from *Q* of about *70[kW/m*^{3}*]*. For c_{pb}*=80[J/(kgK)]* (Figure 3.6) heating is faster and even the temperature higher by *1000K* can be obtained by the storage for a heater power of *25[kW/m*^{3}*]*.

Table 3.3 shows the temperatures to which the energy storage is heated in point 8. (*T2*) for the various powers of the heater *Q* and the specific heat of the modified regolith during the lunar day.

DOI: 10.13009/EUCASS2019-444

Table 3.3: Temperatures at the end of the lunar day in point 8. for different values of c_{pb}

	Q=5000 [W/m^3]	Q=33333 [W/m^3]	Q=60000 [W/m^3]
c_{pb}=80[J/(kgK)]	302.4 [K]	1449.4 [K]	2528.5 [K]
c_{pb}=800[J/(kgK)]	175 [K]	602.2 [K]	1004.1 [K]

This means that the smaller the value of c_{pb} is obtained when modifying the regolith, the smaller will be the required power of the heater to heat the storage.

3.4 The influence of thermal conductivity k_b and specific heat c_{pb} of the energy storage material on the efficiency of the heating process

In order to determine the appropriate parameters of the material from which the storage will be built, two efficiency parameters presented in this chapter were used, the first takes into account the thermal inertia of the material and its heating time, the second – energy used to heat the storage and energy supplied to the system.

3.4.1 Analysis of the efficiency coefficient depending on the thermal inertia of the energy storage and its heating time

Thermal inertia is defined as:

$$I = \sqrt{k c_p \rho} \quad [J/(m^2 K \sqrt{s})] \qquad (3.1)$$

where k is the thermal conductivity *[W/(mK)]*, c_p – specific heat *[J/(kgK)]*, a ρ – density *[kg/m^3]*.

The second parameter, which was used to calculate the coefficient of heating efficiency of the storage, is the heating time of the extreme point (point 8 from fig. 2.1) by *10K*.

This energy storage is expected to have a large thermal inertia and a short time to heat point 8. by 10K. The coefficient described in the following formula was used:

$$eff = \frac{I}{t} \qquad (3.2)$$

where I is the thermal inertia and t – time of heating the point 8. by *10K* [s].

We are looking for such parameters c_p and k to get the largest possible *eff*. A map of this coefficient was generated depending on this parameters in the ranges c_p from *80* to *800[J/(kgK)]* and k from *0.2* to *200 [W/(mK)]*, for heater power *Q=60[kW/m^3]*, and material density ρ=*3000[kg/m^3]*. It is presented in Fig.3.7.

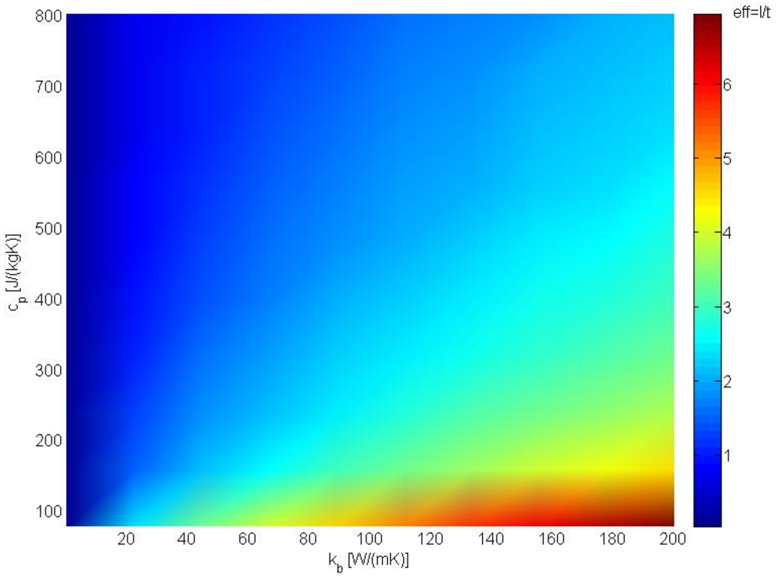

Figure 3.6 Distribution of the value of the efficiency defined by the equation (3.2) depending on the thermal conductivity and specific heat of the modified regolith.

The map shows that high values of the coefficient *eff* appear for high values of thermal conductivity and low of specific heat of the modified regolith.

DOI: 10.13009/EUCASS2019-444

3.4.2 Analysis of the efficiency coefficient depending on energy supplied to the system and used for heating the material of the storage

Finally, the efficiency of the heating process was calculated according to time. Efficiency is defined as:

$$\eta = \frac{E_m}{E_d} \; [10], \qquad (3.3)$$

where: $E_m=\rho c_p \Delta T(t,x,y)$ energy needed to heat the warehouse material to a temperature dependent on time and spatial parameters; $E_d=Qt$ – the thermal energy supplied by the heater multiplied by the heating time.

Obtained efficiency map depending on the parameters is shown in Figure 3.7.

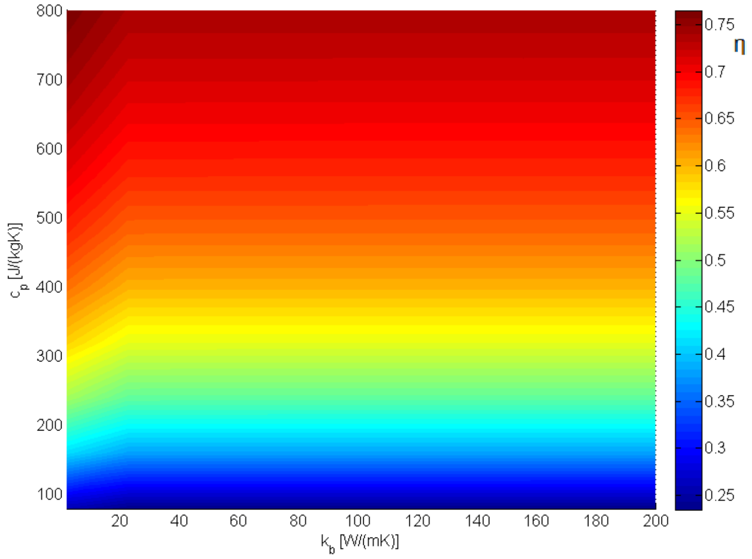

Figure 3.7 Map of the efficiency of the storage depending on the *k* and c_p of the material

Using the above map, a diagram of efficiency η was created depending on time for material parameters $k=2.1[W/(mK)]$ and $c_p=800(J/(kgK)]$ in which the efficiency is the largest. Diagram is shown in Figure 3.8.

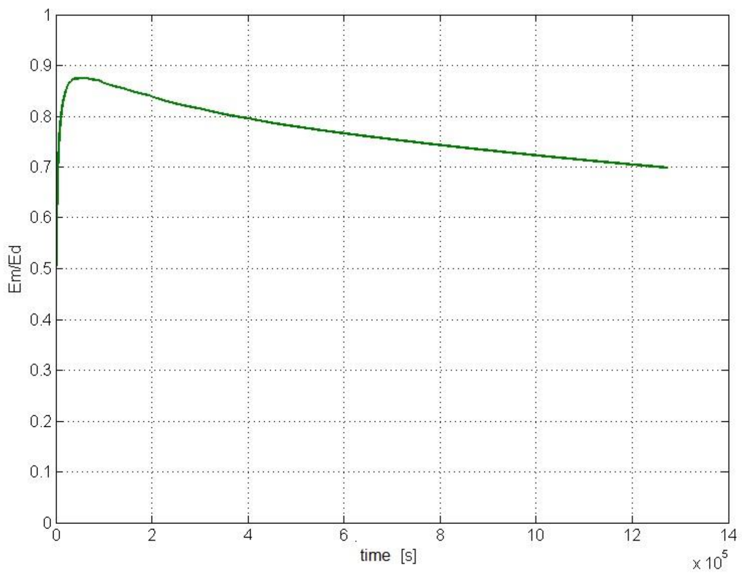

Figure 3.7 The efficiency of the heating process over time.

The efficiency of the process is more than 70% for almost the entire heating period.

The presented maps show that the materials for the analyzed energy storage should have the following parameters $k=200[W/(mK)]$ and $c_p=80[J/(kgK)]$.

However, the calculation of efficiency η shows that a storage made of a material with parameters $k=2.1[W/(mK)]$ and $c_p=800[J/(kgK)]$ will be better.

DOI: 10.13009/EUCASS2019-444

4. Experimental study

As a next step of the research, a number of preliminary experiments were carried out. Samples of material replacing the energy storage were placed in glass beads imitating the native regolith. The samples were then heated and the temperature changes in the system were measured.

4.1 Test-bed

The following elements were used for experiments:
- 4 samples imitating energy storage – made of the WEBER SAINT-GOBAIN EXPRESS concrete in the form of cylinders of various diameters, the bores for the heater were drilled in them – in the axis of the sample and for the sensor – in the middle of the wall; samples are shown in figure 4.1;

Fig.4.1 Tested samples

- small glass balls – as a porous material used as an energy storage surroundings, they are supposed to isolate like the native regolith;
- a heater made of ISOTAN wire with a diameter of *200μm*, wound on a fiber glass cylinder, ISOTAN is characterized by small changes in resistance when changing temperatures, which makes it possible to obtain constant heating power at constant voltage; dimensions of the heater are shown in figure 4.2 with its photo (the device in the picture consists of three heaters, only the middle one was used during the experiment); the heater was powered using a programmable RIGOL DP 1308A power supply device;
- on the same cylinder, a platinum wire with a diameter of *75μm* is wound, which is used to measure the temperature; its resistance was read with the FLUKE digital multimeter.

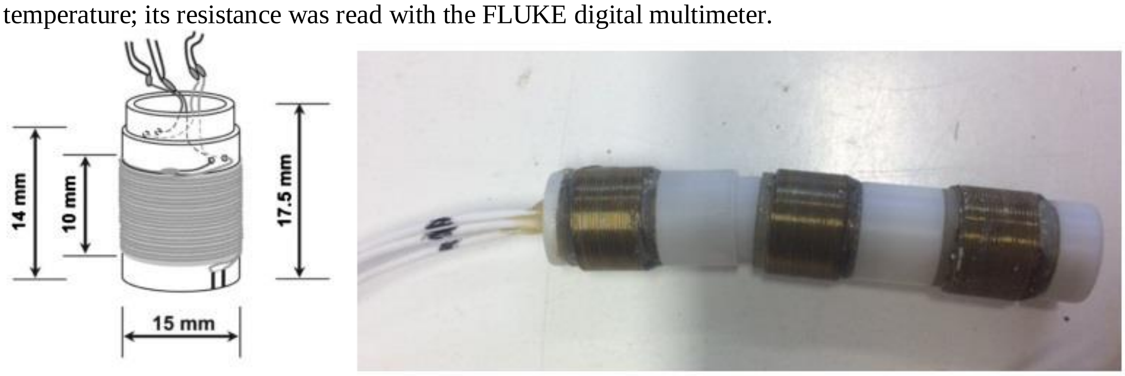

Fig.4.2 Sketch [11] and photo of the used heater

- four Pt100 temperature sensors connected to the Agilent 34970A data logger;
- all elements are placed in an insulated container with a diameter of 220mm.

The scheme of the test-bed is shown in figures 4.3-5.

DOI: 10.13009/EUCASS2019-444

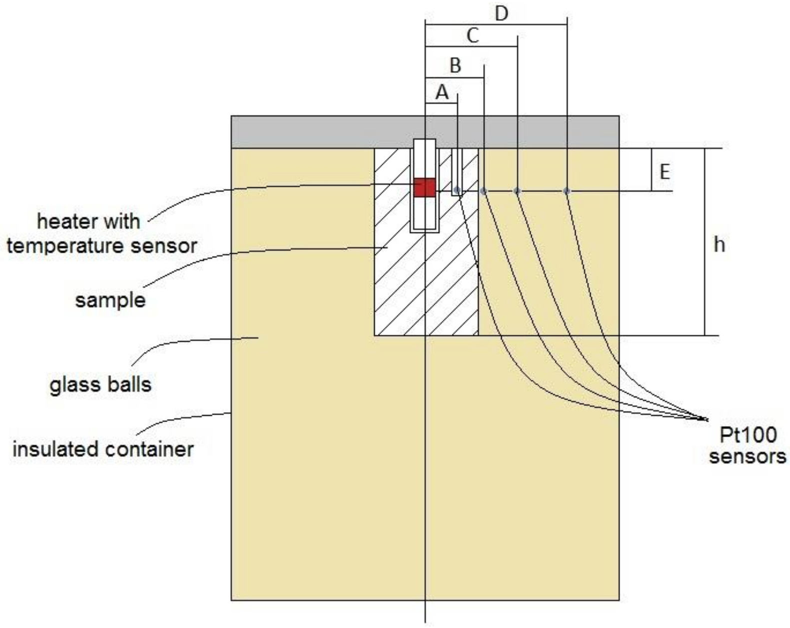

Figure 4.3. Scheme of the test-bed.

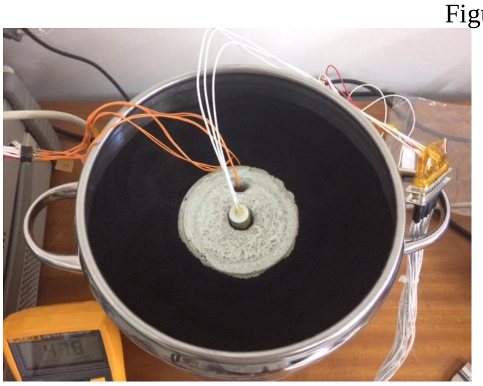

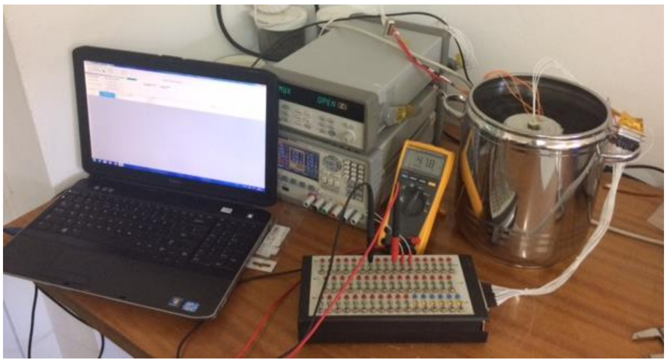

Figure 4.4 and 4.5 Photos of the test-bed.

A measurement was carried out for each of the four samples for the following parameters:

Heating parameters: U = 5V, P = 0.84W

Measurement time: 30 min.

4.2 Results

Temperature charts in the system were obtained depending on time, an example of this chart for all sensors is shown in Fig 4.6.

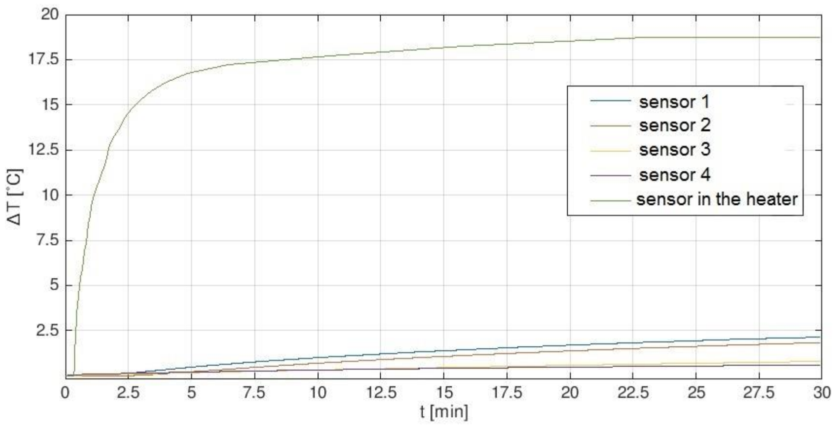

Figure 4.6. Temperature changes in one of the samples

DOI: 10.13009/EUCASS2019-444

It is visible that the sensor in the heater recorded much larger temperature changes than the rest of the sensors. This is due to the fact that the diameters of holes drilled in the samples were slightly larger than the diameter of the heater, so that it could be placed inside. Inaccurate contact between the heater and the material of the sample causes a large thermal resistance. More specifically, the temperature changes recorded by the Pt100 sensors are shown in figure 4.7.

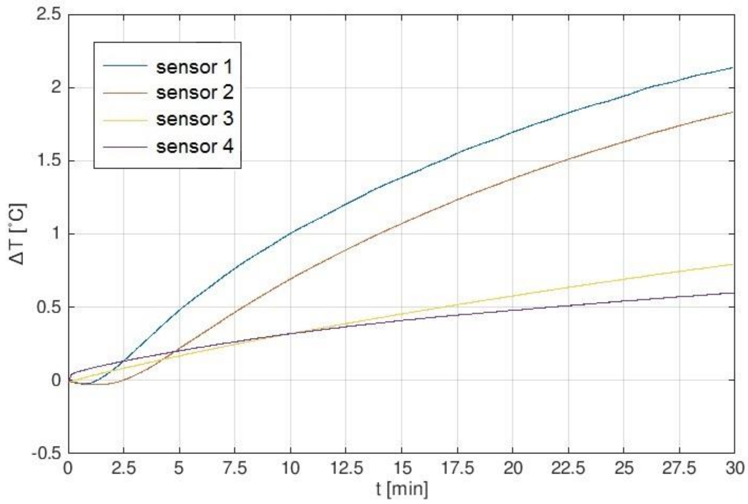

Figure 4.7. Temperature changes in one of the samples.

The graph clearly shows that sensors 1 and 2 (blue and red lines) located in the bore and on the surface of the sample recorded larger temperature changes than the other two sensors placed in the surrounding glass balls.
Temperature differences recorded by sensors 3 and 4 (yellow and purple lines) in the tests of all samples are small – between 0.3 and 0.7 ˚C.

4.1 Findings

Heating of four cylindrical samples of different diameters were tested and the following conclusions were obtained:

- The sample material heats up more than the glass balls used as an insulating porous material.
- Large temperature differences between the heater and the heated material of the samples result in part from the thermal resistance of the samples themselves and partly from inaccurate contact between the heater and sample as well as the sample and sensors, the dusty layer covering the surface of the holes after drilling and the imperfections of the material itself.

Further experiments could include:

- testing of samples surrounded by the AGK-2010 regolith analogue, produced by CBK PAS and AGH,
- examination of samples made of a material with better thermal properties – e.g. basalt.

5. Conclusions

In this work, the possibility of determining the parameters of the thermal energy storage material in order to maximize the efficiency of the heating the process of in lunar conditions was confirmed.

Based on previous analyzes of the thermal energy storage system on the Moon [7], the thermal mass model was made, it was to be made of modified lunar regolith in order to minimize mission costs. A series of simulations were carried out to obtain information on the influence of the material parameters of the storage material and the thermal contact conductivity at the interface of storage material and the surrounding native regolith on the temperatures in the heated system and time and efficiency of the heating process. It has been proven that the native regolith layer can effectively isolate the storage placed under the surface against large temperature amplitudes on the surface of the Moon. Study has also indicated that some of the energy from the heated storage penetrates into the surrounding regolith despite a large difference in the conductivity of materials and that with the increase of the heater's power, the temperature difference at the interface between materials increases.

The analysis of the influence of thermal contact conductivity at the materials interface h shows that it should be as small as possible to allow as much energy as possible remain in the storage. Simulations carried out for different

DOI: 10.13009/EUCASS2019-444

values of thermal conductivity c_p have shown that for smaller values of this parameter, a shorter heating-up time of the storage can be achieved or a lower power heater can be used. Analyzes of the efficiency of the storage heating process indicated that the first adopted coefficient – depending on the thermal inertia and the heating time of the storage achieves the highest values for parameters $k=200[W/(mK)]$ and $c_p=80[J/(kgK)]$ and the second coefficient depends on the energy used for heating the storage and delivered to the system and indicates that the values $k=2.1[W/(mK)]$ and $c_p=800[J/(kgK)]$ will allow the greatest efficiency.

In addition to simulation analyzes, simple experimental tests were performed by heating concrete samples surrounded by glass balls. The temperature distributions in the system were examined and it was proven that the sample material heats up to higher temperatures than glass balls. There were significant differences in temperature between the heater and the heated material of the samples resulting from inaccurate contact between the heater and the sample as well as the sample and used sensors, and the imperfection of the sample.

The described research proves that it is possible to select the appropriate material parameters to make an energy storage using the simulation and experimental tools used for analyzes.

Further research can include the performance of experimental tests on samples with better thermal properties, surrounded by the AGK-2010 regolith analogue. Knowing the exact parameters of the materials used in the tests, one could perform simulations based on them in the COMSOL and MATLAB software, and then compare the results of simulation and experimental tests. Then, analysis of heat collection from the storage will also be needed. The next step in the analysis of the storage could be the development of methods for processing the AGK-2010 regolith analog proposed in the literature, such as compressing or sintering and thermal testing of samples obtained in this way.

References

[1] The Global Exploration Strategy: The Framework for Coordination. 2007. https://www.nasa.gov/pdf/296751main_GES_framework.pdf, access: 06.2019

[2] Sanders G.B., Larson W.E. 2013. Progress Made in Lunar In-Situ Resource Utilization under NASA's Exploration Technology and Development Program. NASA.

[3] NASA. 2005. NASA Capability Roadmaps Executive Summary.

[4] NASA. 2015. NASA Technology Roadmaps TA 7: Human Exploration Destination Systems.

[5] Balasubramaniam R. at al. 2009. Analysis of solar-heated thermal wadis to support extended-duration lunar exploration, AIAA

[6] Balasubramaniam R at al. 2009. An Extension of Analysis of Solar-Heated Thermal Wadis to Support Extended-Duration Lunar Exploration, Journal of Thermophysics and Heat Transfer.

[7] Climent B. at al. 2014. Heat storage and electricity generation in the Moon during the lunar night. Acta Astronautica.

[8] Taylor L., Meek T. 2015. Microwave Sintering of Lunar Soil: Properties, Theory, and Practice. ASCE.

[9] Heiken G., Vaniman D., French B. 1991. Lunar Sourcebook. Lunar Planetary Institute.

[10] Dincer I., Rosen M. 2011. Thermal Energy Storage Systems and Applications. Wiley.

[11] Kömle at al. 2011. *In situ* methods for measuring thermal properties and heat flux on planetary bodies. Planetary and Space Science 59:639-660.